Selective benefits of damage partitioning in unicellular systems and its effects on aging

N. Erjavec[a,1], M. Cvijovic[a,b,1], E. Klipp[b,c,2], and T. Nyström[a,2]

[a]Department of Cell and Molecular Biology, Göteborg University, Medicinaregatan 9C, 413 90 Göteborg, Sweden; [b]Max-Planck Institute for Molecular Genetics, Ihnestrasse 73, 14195 Berlin, Germany; and [c]Department of Theoretical Biophysics, Humboldt University Berlin, Invalidenstrasse 43, 10115 Berlin, Germany

Edited by Rodney Levine, National Heart, Lung, and Blood Institute, Bethesda, MD, and accepted by the Editorial Board September 29, 2008 (received for review May 9, 2008)

Cytokinesis in unicellular organisms sometimes entails a division of labor between cells leading to lineage-specific aging. To investigate the potential benefits of asymmetrical cytokinesis, we created a mathematical model to simulate the robustness and fitness of dividing systems displaying different degrees of damage segregation and size asymmetries. The model suggests that systems dividing asymmetrically (size-wise) or displaying damage segregation can withstand higher degrees of damage before entering clonal senescence. When considering population fitness, a system producing different-sized progeny like budding yeast is predicted to benefit from damage retention only at high damage propagation rates. In contrast, the fitness of a system of equal-sized progeny is enhanced by damage segregation regardless of damage propagation rates, suggesting that damage partitioning may also provide an evolutionary advantage in systems dividing by binary fission. Indeed, by using *Schizosaccharomyces pombe* as a model, we experimentally demonstrate that damaged proteins are unevenly partitioned during cytokinesis and the damage-enriched sibling suffers from a prolonged generation time and accelerated aging. This damage retention in *S. pombe* is, like in *Saccharomyces cerevisiae*, Sir2p- and cytoskeleton-dependent, suggesting this to be an evolutionarily conserved mechanism. We suggest that sibling-specific aging may be a result of the strong selective advantage of damage segregation, which may be more common in nature than previously anticipated.

computational modeling | protein damage | fitness | asymmetry

The division of labor between somatic cells and germ cells may be one reason why young individuals of both animals and plants start off with low levels of protein damage. Germs cells, in contrast to somatic cells, are optimized for eternal youthfulness (1, 2) which may be achieved by (*i*) germ cells enjoying elevated, or more functional, homeostatic maintenance systems (3); (*ii*) an asymmetrical partitioning of damage during gametogenesis (4); and/or (*iii*) a selection process that rids the organisms of germ cells exhibiting high levels of damage (5). Yet another possibility is that germ cells are provided with superior means to rid themselves of damaged proteins but are not doing so until embarking on embryonic development (6) such that resources for damage elimination are only invested in the cells that will become progeny.

There is no distinction between somatic and germ line cells in unicellular organisms, yet some unicellular microbes display lineage-specific aging and a division of labor between the cells produced during cytokinesis. For example, in the budding yeast *Saccharomyces cerevisiae* (7) one of the sibling cells (the larger mother cell) undergoes age-related changes and, with repeated divisions, eventually loses its capacity to undergo further cytokinesis. Yet the aging mother cell is capable of generating daughter cells, arguably a sort of yeast counterpart to germ line cells, with a full replicative potential (8–11). This generation of small and young progeny from large and old progenitor cells encompasses a process limiting the inheritance of toxic and deteriorated material, such as extra chromosomal rDNA circles (ERCs) (8) and oxidatively damaged (carbonylated) and aggregated proteins (10, 12, 13) by the progeny. Another asymmetrically dividing microorganism, the bacterium *Caulobacter crescentus*, also displays a division of labor and lineage-specific aging (14). In fact, the benchmark for cellular symmetry, the bacterium *Escherichia coli*, likewise shows signs of replicative aging in a lineage-specific manner (of course, there is no cell division that is perfectly symmetrical when, for example, the age of DNA strands and cell poles is taken into consideration) (15). Therefore, it is possible that unicellular systems partition labor between the cells produced upon cytokinesis, analogous to the division of labor observed between the soma and germ line of higher organisms (16).

These observations raise questions regarding the ultimate and proximate causation of fitness asymmetry in a unicellular system: Is there an advantage to producing cells of different size, different levels of damage, and unequal reproductive potential? To approach these questions, we developed a mathematical model aimed at elucidating effects of cellular asymmetries on fitness, proliferating capacity, and aging, and we used *Schizosaccharomyces pombe* dividing by binary fission to test predictions of the model.

Results

Modeling Growth and Cell Division. To simulate the proliferation of a simple entity consisting of 2 types of molecules (e.g., diffusible proteins), intact and damaged ones, we constructed a mathematical model based on ordinary differential equations (see Eqs. **1–6**), describing the accumulation of the intact (P_{int}) and damaged (P_{dam}) proteins, such as oxidatively carbonylated proteins, during the cell cycle and successive cell generations. The sum (P) of intact (P_{int}) and damaged (P_{dam}) proteins determines the total size of the entity. The temporal dynamics of P_{int} are given by a production term (rate of protein synthesis; maximal rate k_1/k_s), that depends on the current amount of total protein in the cell, the rate of intact protein degradation (rate constant k_2), and the conversion of intact proteins to irreversibly damaged proteins (rate constant k_3) (ref. 1; see *Materials and Methods*). The constant k_s represents the protein concentration leading to half-maximal protein production rate. The dynamics of P_{dam} are ruled by the conversion of intact proteins to damaged proteins (k_3) and the rate of degradation of damaged proteins (rate constant k_4). Initially, the number of intact and damaged molecules increase until production and degradation is balanced (Fig. S1 *A* and *B*). It has been estimated that as much as one-third of every protein in some organisms may be damaged by carbonylation, a specific irreversible oxidative modification (17).

Author contributions: N.E., M.C., E.K., and T.N. designed research; N.E. and M.C. performed research; N.E., M.C., E.K., and T.N. analyzed data; and N.E., M.C., and T.N. wrote the paper.

The authors declare no conflict of interest.

This article is a PNAS Direct Submission. R.L. is a guest editor invited by the Editorial Board.

[1]N.E. and M.C. contributed equally to this work.

[2]To whom correspondence may be addressed. E-mail: thomas.nystrom@cmb.gu.se or klipp@molgen.mpg.de.

This article contains supporting information online at www.pnas.org/cgi/content/full/0804550105/DCSupplemental.

© 2008 by The National Academy of Sciences of the USA

Downloaded at Palestinian Territory, occupied on December 31, 2021

www.manaraa.com

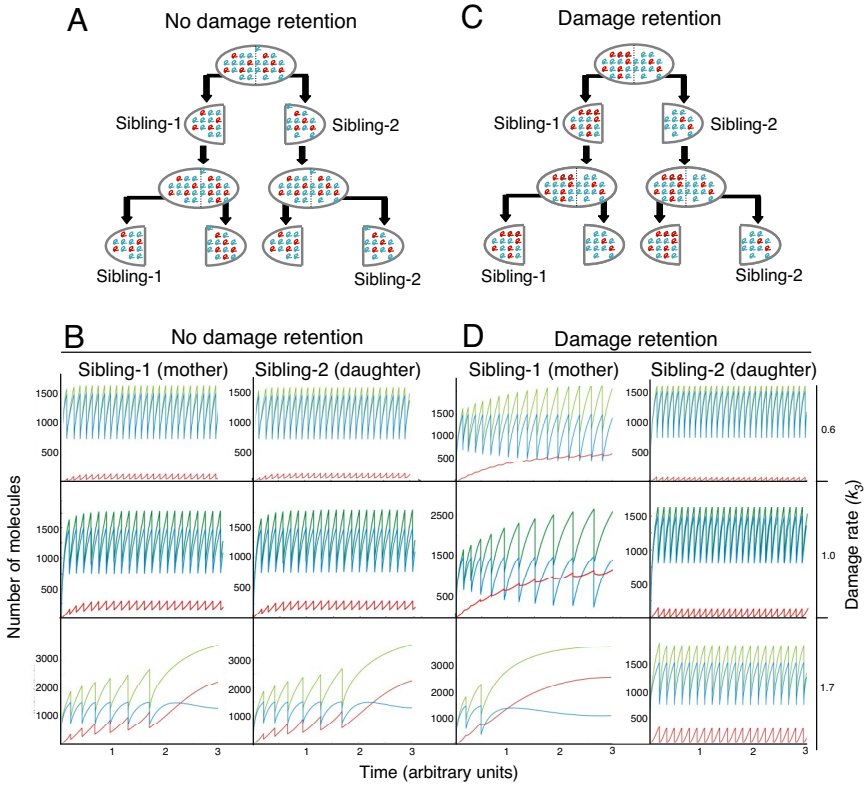

Fig. 1. Damage segregation prevents clonal senescence of a symmetrically dividing system. (*A* and *C*) Schematic representation of a symmetrically dividing system, the sibling lineages analyzed, and the distribution of intact (blue) and damaged (red) proteins in a system without (*A*) and with (*C*) damage segregation. (*B* and *D*) Simulations of divisions, accumulation of intact (blue), damaged (red), and total (green) proteins during progressive cell cycles in the sibling lineages 1 and 2 at different rates of damage production (k_3). Simulations were performed without (*B*) and with (*D*) segregation of damage. The temporal dynamics of cytokinesis, damaged, intact, and total proteins at low ($k_3 = 0.6$; *Top*), moderate ($k_3 = 1.2$; *Middle*), and high damage ($k_3 = 1.7$; *Bottom*) production rates are shown. The retention coefficient used in *D* is 0.875.

Based on this information and taking other noxious modifications into consideration, we tested P_{dam} damaging rates generating up to 66% damage (of total protein). The half-life of proteins in unicellular systems has been shown to range from minutes to days depending on the specific protein analyzed, but most bulk proteins display half-lives markedly longer than a generation time (see ref. 18). Therefore, in the present study we simulated between 5% and 35% degradation of total proteins within 1 generation. Protein and RNA syntheses in *S. pombe* have been shown to increase exponentially during the cell cycle (19), whereas volume increase is biphasic linear (20). The model has therefore been tested for both types of growth, yielding comparable results (Fig. S1 *A* and *B*).

To trigger cell division in the growing entity, we introduced a critical value P_{div} that defines the number of intact proteins required for cytokinesis, including all checkpoints from initiation of cell division to completion of cytokinesis. We made the assumption that the critical cell size reflects the accumulation of key proteins and that these proteins are, on average, as susceptible to damage as bulk protein. The damaged proteins exhibit no intrinsic value of toxicity, but their accumulation increases the generation time by affecting the time it takes for the cell to reach the critical, functional, and undamaged size required for cytokinesis (P_{div}) (Eq. **1**). When P_{div} has been reached, the system can divide in a symmetrical or asymmetrical fashion with respect to size and damaged proteins (Fig. 1 *A* and *C* and Fig. S2 *A* and *C*). A set of transition equations determines the size of the cells produced and how the proteins are distributed between progenitor and progeny during cytokinesis (see *Materials and Methods*).

Effects of Asymmetry on Clonal Senescence. The model was initially simulated for low damage rates k_3 (see *Materials and Methods*), with an equal inheritance of damaged proteins (Fig. 1*A*). Under these conditions the system was characterized by constant initial and final concentrations of intact and damaged proteins during successive generations and the population was immortal (Fig. 1*B*). At moderate damage rates, cells still divided indefinitely but displayed longer generation times (Fig. 1*B*). At high damage rates, the cells went through a finite number of divisions characterized by progressively longer generation times and a pronounced accumulation of damaged proteins at the expense of intact ones, eventually preventing P_{div} from being attained (Fig. 1*B*). Because division, in this simulation, was perfectly symmetrical and all cells in the population were identical, the outcome was clonal senescence. That is, the model predicted that, at high damage rates, the entire population would eventually reach a "dead end," reminiscent of the Hayflick limit (21).

We next asked whether an unequal distribution of damaged proteins during cytokinesis (Fig. 1*C*) among individuals affects the damage rate at which clonal senescence is reached. We therefore introduced the retention coefficient into the model (see Eqs. **7** and **8** in *Materials and Methods*); such that equal-sized siblings were distinguishable by the amount of damaged proteins they inherited. The system then showed signs of sibling-specific replicative senescence; the cells that retained more of the damage displayed progressively longer generation times, whereas the "low-damage" sibling lineage propagated indefinitely (Fig. 1*D*). In addition, damage segregation (Fig. 1*D*) allowed the population to propagate at damage rates, which caused clonal senescence of a perfectly symmetric system (Fig. 1*B*).

This analysis was followed by testing whether a difference only in size between a large progenitor and a smaller offspring (Fig. S2*A*)

Downloaded at Palestinian Territory, occupied on December 31, 2021

www.manaraa.com

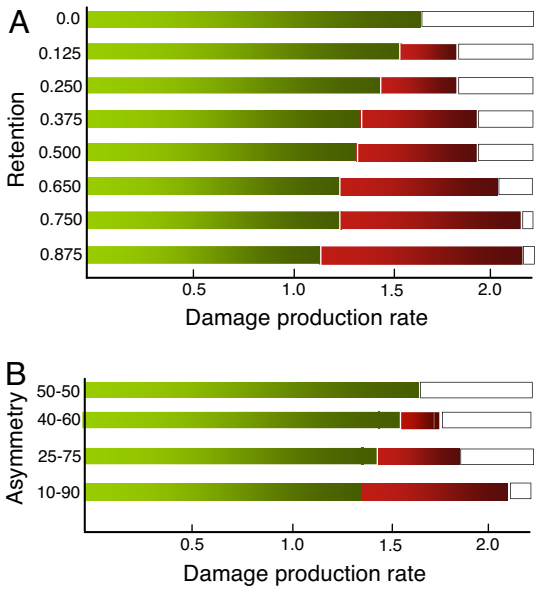

Fig. 2. Damage segregation and size asymmetry causes sibling-specific aging but increases the robustness of the system. (*A*) Effect of damage segregation (*y* axis) on damage levels (k_3; *x* axis) triggering clonal senescence and replicative aging. Green bars indicate that both siblings produced during cytokinesis are immortal but exhibit longer generation times with increasing damage. Red bars indicate that the sibling retaining more damage at the time of cytokinesis undergoes replicative senescence; i.e., can only perform a finite number of new generations, whereas the other sibling is immortal. Empty bars indicate that the system has reached clonal senescence; i.e., a damage rate at which both siblings display a finite ability to produce new cells. (*B*) Effect of size asymmetry (*y* axis) on damage levels (k_3; *x* axis) triggering clonal senescence and replicative aging. Color-coding is as described in *A*.

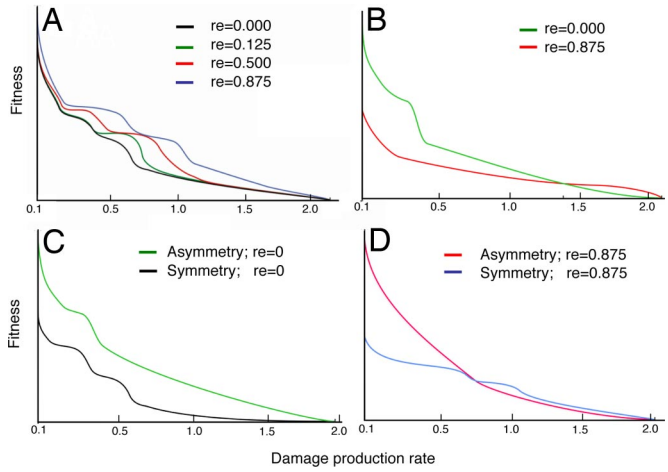

Fig. 3. Effects of asymmetries on population fitness upon increasing rates of damage production. Fitness, defined by the population size produced within one time unit (*y* axis), is plotted as a function of increasing damage rate (k_3; *x* axis). The different retention coefficients modeled are color-coded and shown in the graph. (*A*) Fitness of symmetrically dividing systems (by size) displaying different degrees of damage segregation as indicated. (*B*) Fitness of an asymmetrically dividing system (by size) displaying no retention (green) and retention (red). (*C*) Fitness of a symmetrically dividing system without damage retention (black) compared with an asymmetrically dividing system without damage retention (green). (*D*) Fitness of a symmetrically dividing system with damage retention (blue) and an asymmetrically dividing system with the same degree of damage retention (red).

was sufficient to prevent clonal senescence. At low to moderate damage, the system showed signs of a sibling-specific replicative senescence, typical of asymmetrical dividing systems such as budding yeast. The larger parent lineage (mother cell) displayed increasingly longer generation times (Fig. S2*B*) until eventually the persistent titration of intact proteins by damaged proteins prevented it from dividing again. In contrast, at the same damage rate, the smaller progeny lineage continued to divide indefinitely (Fig. S2*B*). Also, a system of different-sized progeny can proliferate ad infinitum even without damage segregation at damage rates giving rise to clonal senescence in the perfectly symmetrical system (Fig. 1*B* and Fig. S2*B*). When damage was segregated such that the larger mother cells received an even higher load than expected from their size (Fig. S2*C*), the system could withstand even higher levels of damage before entering clonal senescence (Fig. S2*D*).

The model also suggested that, to prevent clonal senescence, the degree of damage segregation (or size asymmetry) needed to increase as the damage production rate was elevated (Fig. 2 *A* and *B*). The tradeoff for this beneficial effect of damage retention or size asymmetry on clonal senescence is sibling-specific aging at progressively lower damage rates (Fig. 2 *A* and *B*). Interestingly, even very low retention coefficients ($re = 0.125$; 1 sibling effectively retaining 58% of the overall P_{dam}) were sufficient to prevent a symmetrically dividing population from reaching a dead end at moderate damage rates (Fig. 2*A*).

Effects of Asymmetry on Population Fitness. If we define fitness as the number of entities produced in total per time unit, the population fitness of the different systems can be calculated at different damage production rates. When doing so for a system that divided symmetrically size-wise, damage segregation surprisingly improved population fitness at all damage rates analyzed (Fig. 3*A*). Different models by Ackerman *et al.* (22) and Watve *et al.* (23) describing the effects of differentiation between an aging parent and rejuvenated offspring in a population of unicellular organisms also suggested benefits of damage segregation at least at one fixed level of damage.

In a system with different-sized progeny, damage partitioning (based on the model and assumptions made) is only beneficial at high damage propagation rates (Fig. 3*B*). On the other hand, a population dividing asymmetrically will present a substantial fitness advantage over one dividing symmetrically at all damage rates (Fig. 3*C*). However, if damage is segregated, an asymmetrical system is favored at low damage but looses out at high damage (Fig. 3*D*) due to the fact that larger parent cells will reach the size for division (P_{div}) much faster than their symmetrically dividing counterparts (Fig. 1 and Fig. S2). The fact that the smaller progeny have a longer generation time does not outweigh the parents' rate as long as the proportion of intact constituents is sufficiently high. However, as the damage rate increases, the progenitor lineage slows down, making the fitness largely dependent on the smaller offspring. At this point, the beneficial effect of retention allows a symmetrically dividing population with retention to be equally well off, or overtake, an asymmetrically propagating population (Fig. 3*D*).

Damage Segregation in a System Dividing by Binary Fission. Our simulations suggest that a system dividing symmetrically by size displays an increased fitness at all damage propagation rates when partitioning its damage during cytokinesis. This suggestion raises the possibility that segregation is more common than previously anticipated, which prompted us to analyze the in situ distribution of carbonylated proteins in the fission yeast, *S. pombe*. Although the volume of the 2 siblings is equal, previous landmarks of division (birth scars) will remain confined to one-half of the growing cell and be inherited by one "sib" only (20) (Fig. 4*A*). When we followed birth scars and protein carbonyls during the cell cycle in synchronized cells, we found that carbonylated proteins were inherited asymmetrically between the 2 siblings such that the one with the previous birth scar was always left with more damage (Fig. 4*B*).

Downloaded at Palestinian Territory, occupied on December 31, 2021
www.manaraa.com

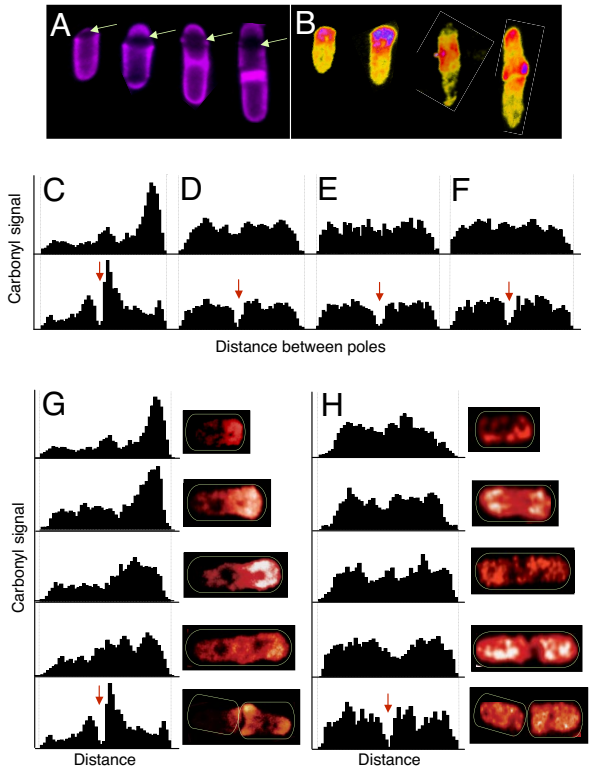

Fig. 4. Damaged proteins are segregated during binary fission of *S. pombe* in a Sir2p- and Tea1p-dependent way. (*A*) Localization of septum and birth scar(s), visualized with calcofluor white, in cells of *S. pombe* during progression through the cell cycle. Arrows indicate the birth scar. (*B*) Distribution of carbonylated proteins during the cell cycle. In situ preparation and detection of carbonyls was carried out as described in *Material and Methods* and the cells placed such that the pole displaying the birth scar was on top. The cells were synchronized by centrifugal elutriation, resuspended in YES media and subsequently allowed to grow at 30 °C. After synchronization, ≈30–40 cells were analyzed at each state in the cell cycle. Carbonyls were detected and quantified in situ as described in *Material and Methods*. Blue and purple denote the highest concentration of carbonyls followed by red and yellow. (*C*) Quantification of carbonyls from pole to pole in newborn wild-type cells (*Upper*) and cells immediately before cell division (*Lower*). The spatial intensity of the carbonyl signal was obtained by drawing a line along the longitudinal axis of the cells and deriving the corresponding intensity plot profile. Approximately 30–40 cells were analyzed at each state in the cell cycle. (*Lower*) The red arrow points to the site of the septum. (*D*) Quantification of carbonyls from pole to pole in newborn *tea1*Δ cells (*Upper*) and cells immediately before cell division (*Lower*). (*E*) Quantification of carbonyls from pole to pole in newborn wild-type (*Upper*) and cells immediately before cell division (*Lower*) transiently treated with Lantranculin-A as described in *Materials and Methods*. (*F*) Quantification of carbonyls from pole to pole in newborn wild-type (*Upper*) and cells immediately before cell division (*Lower*) transiently treated with Benomyl as described in *Materials and Methods*. (*G* and *H*) Quantification of carbonyls from pole to pole during the cell cycle of wild-type (*G*) and *sir2*Δ (*H*) cells. Representative micrographs of cells at the different stages of the cell cycle are depicted next to the quantification graphs. The red arrow points to the site of the septum.

After completion of cytokinesis, the newborn cells displayed most of their damage at the new end (Fig. 4 *B* and *C*).

Growth of *S. pombe* will first take place at the old end and subsequently also at the new end (damage-enriched). The latter growth period is called New End Take Off (NETO) (20, 24). NETO is characterized by the reorganization of the actin cytoskeleton and a redistribution of actin patches from the ends toward the equatorial plane of the cell (24), similar to the redistribution of damage shown here. We found that Tea1p, a protein required for establishing cell polarity (25, 26) and the redistribution of actin patches during

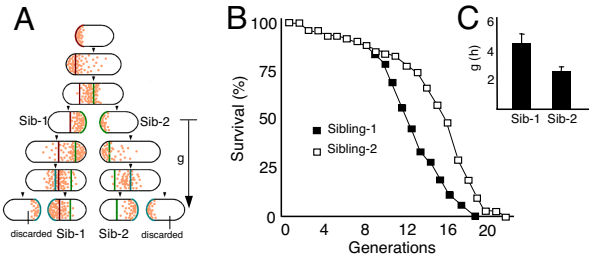

Fig. 5. *S. pombe* display sibling-lineage specific aging. (*A*) Schematic representation of the criteria used in discriminating between ''old'' (Sib-1) and ''new'' (Sib-2) siblings, derived from a common 9-generations-old progenitor (starting cell). Vertical bars indicate birth scars, present as bulges on the cell surface, and here represented chronologically by different colors. Upon division, the cell with more birth scars (i.e., more divisions) and rounder appearance was selected as the older sibling. These cells coincide with those inheriting more carbonylated proteins, as detected by immunofluorescence microscopy and here depicted by orange dots. The arrow denotes the generation time (*g*) as analyzed for the 2 siblings and presented in *C*. (*B*) Replicative life span of the old sibling (Sibling-1; filled squares; $n = 75$), and new sibling (Sibling-2; open squares; $n = 75$) derived from a common 9-generations-old progenitor cell. (*C*) Generation times for old (Sib-1) and new (Sib-2) siblings.

NETO, is necessary also for the polar localization of damage and the redistribution of damage toward the equatorial plane before cytokinesis (Fig. 4*D*). In addition, as with budding yeast, the mechanism responsible for the asymmetric segregation of damaged proteins in *S. pombe* is cytoskeleton-, actin-, and microtubule-dependent (Fig. 4 *E* and *F*). Intriguingly, deleting *SIR2*, which has been shown to be a requirement for establishing damage asymmetry in budding yeast (10, 12, 13), resulted in the same loss of spatial control and retention of carbonylated proteins as treatment with cytoskeleton depolymerizing drugs (Fig. 4 *G* and *H*).

Because our model predicted that symmetrically dividing cells without protein damage retention would display a reduced fitness and run into clonal senescence at lower damage rates than cells partitioning their damage, we monitored growth of wild-type and *sir2*Δ mutant cells at different concentrations of hydrogen peroxide. Interestingly, whereas wild-type and *sir2* mutant populations display the same fitness (growth rate) when cultured without stressors, hydrogen peroxide caused a much more pronounced fitness reduction in *sir2* mutants than wild-type cells (Fig. S3). However, we cannot presently assign the fitness reduction and stress sensitivity of *sir2* mutant cells to their inability to segregate damage because a number of other functions, including silencing at different loci, are severely affected in the mutant.

We next followed the replicative potential of both *S. pombe* sibling lineages, arising from a common parent cell, which had already completed 9 divisions and therefore accumulated damaged proteins (see Fig. 5*A* and *Materials and Methods*). We found that the sibling enriched for protein damage (“old” sib) displayed a shorter mean life span (12.5 generations) than the “young” sib (15.9 generations; see Fig. 5*B*), Moreover, the generation time of the damage-enriched cell was markedly longer; 4.5 h compared with 2.5 h for the new sib (Fig. 5*C*). This result points to a “sibling-specific” aging in *S. pombe* that correlates with the unequal inheritance of damaged proteins.

Discussion

The models constructed in this work predict that, in a proliferating system, there is a maximum rate of damage the system can tolerate, beyond which the proportion of intact constituents becomes insufficient for the cell to carry out any further division. In a completely homogeneous population, this point is marked by the simultaneous death (or proliferation-arrest) of all individuals; i.e., clonal senescence (Fig. 1*B*). Interestingly, it has been shown experimentally that

Downloaded at Palestinian Territory, occupied on December 31, 2021

www.manaraa.com

mouse embryonic fibroblasts do not senesce when cultivated under low oxygen tension (3%) but do so at high oxygen tension (20%) (27). In addition, lowering superoxide production by mild mitochondrial uncoupling delays replicative senescence of human fibroblasts (28). However, the potential role of protein damage has, so far, not been considered in these systems. The entities of a population could potentially avoid clonal senescence by reducing the rate of conversion of intact proteins to damaged proteins (k_3) or increasing the rate of their removal (k_4); i.e., by increasing their investment in classical maintenance and quality control pathways. However, the simulations suggest that there are other means of preventing a cell population from reaching clonal senescence, chiefly by diversifying individuals within the population. This strategy can be achieved either by unequal partitioning of damage during cytokinesis or producing progeny of different size. In either case, this diversification of individuals leads to lineage-specific aging. This notion is in line with the views of Partridge and Barton (29) and Kirkwood (30), who considered potential benefits of asymmetry in simple unicellular systems and how this might develop into aging. Interestingly, it was recently shown that differential fitness of *E. coli* siblings is associated with an unequal partitioning of protein aggregates (31). In addition, when transient external stresses reach lethal levels, an asymmetrical segregation of irreparable damage and/or size asymmetry may permit survival of the clone at the expense of the "mother-type" cells in which the damage is retained.

The model suggests that even very low retention coefficients (e.g., a scenario where one cell receives 58% and the other 42% of the damage) may have a great impact on the system's ability to escape clonal senescence, at least at moderate damage rates. Such small differences in damage inheritance may be a consequence of stochastic variance rather than an evolved strategy for generating asymmetry. However, as the damage rate increases, the damage retention, or size asymmetry, needs to be more pronounced than can be afforded by stochasticity, and a more deterministic mechanism for generating asymmetry thus appears to be required to escape clonal senescence. In addition, when the total fitness (number of cells produced per time unit) of the systems is considered, damage retention may be a mixed blessing. For example, when considering a different cell-size organism like budding yeast, damage retention will push the upper limits for how much damage the system can endure before entering clonal senescence (Fig. 2) but becomes a selective disadvantage at low damage production rates (Fig. 3). This problem raises the question of whether the efficiency of damage segregation could be adjusted with changing environmental demands. Interestingly, damage segregation in budding yeast becomes more pronounced after increased oxidative stress (10). In addition, unusually poor growth conditions elicit a switch from a morphologically symmetrical to a more asymmetrical type of division in fission yeast (32), indicating that this organism also displays a dynamic ability to break-up symmetry on environmental demands.

We believe the data reported here raise the possibility that "sibling-specific" aging and "rejuvenation" in unicellular systems may have evolved as "by-products" of a strong selection for damage segregation during cytokinesis. A question of interest is whether such division of labor between cells undergoing division is retained also in multicellular organisms, for example during the generation of germ line cells or cellular differentiation.

Materials and Methods

Strains. All strains used in this study were isogenic or derivatives of the 972h$^-$ wild type (33). The *sir2*Δ and *tea1*Δ mutants were derived from strain sp286 (ade6–210 ura4-D18 leu1–32 h$^+$) and had the gene of interest replaced by a KanMX4 cassette.

Immunofluorescence. Cells were grown to OD_{600} = 0.7 in YES medium (1% yeast extract, 3% glucose) and synchronized by centrifugal elutriation using a JE5 rotor (Beckman–Coulter) so that those with a length of <9 μm were collected at 312 × *g* and 45 mL/min. The cells collected were resuspended in YES and allowed to grow at 30 °C. Aliquots were taken thereafter and stained with calcofluor white (20) to determine septum and birth scar location. In situ preparation and detection of carbonyls was carried out as described previously (10, 34). Approximately 30–40 cells were analyzed for each sample.

Treatment with Latrunculin A (Wako) and Benomyl (Fluka) was carried out as previously described (35, 36), and costaining with DAPI and Fluorescein-Phalloidin (Molecular Probes) was performed in accordance with previous protocols (34).

Lifespan Analysis. Wild-type cells were placed and allowed to divide once, at which point the sibling devoid of birth scars was kept, and its sister was discarded. This "virgin" sib was then followed for 9 successive generations, by removing the "scar-free" sister sibs generated at every division (37). Then both siblings were isolated: The sibling with the greater number of birth scars and roundest appearance was defined as the "old" sib, whereas its more regularly shaped scar-free counterpart was defined as the "new" sib. The replicative potential and generation time of these 2 sibs were then followed independently.

Model Description. The ordinary differential equations (see Eq. **1**) describe the behavior of intact (P_{int}) and damaged (P_{dam}) proteins, such as oxidatively carbonylated proteins (17), during the cell cycle and successive cell generations.

$$\begin{aligned}\frac{dP_{\text{int}}}{dt} &= \frac{k_1}{k_s + P_{\text{int}} + P_{\text{dam}}} - k_2 P_{\text{int}} - k_3 P_{\text{int}}\\ \frac{dP_{\text{dam}}}{dt} &= k_3 P_{\text{int}} - k_4 P_{\text{dam}}\\ \frac{dP}{dt} &= \frac{k_1}{k_s + P_{\text{int}} + P_{\text{dam}}} - k_2 P_{\text{int}} - k_4 P_{\text{dam}}\end{aligned} \quad [1]$$

Initially, all protein concentrations rise until production and degradation is balanced, (Fig. S1 *A* and *B*). To trigger cell division in the growing system, we introduced a critical value P_{div}, that defines the number of intact proteins required for the cell to initiate cytokinesis. P_{div} should be well below the value reached by the system at steady state and was arbitrarily set here to 1,500 molecules per entity. For the sake of simplicity, $k_2 = k_4 = \ln 2$ [from half-life ($t_{1/2}$) defined as ln2/k for $t_{1/2} = 1$]. To simulate different rates of conversion, k_3 is given a range of values, from 0.1 to 2.2. k_1 has been adjusted by hand allowing for a steady state to be reached and has been assigned a final value of 10^7. Parameters were implemented to resemble known values describing cell growth, protein synthesis and degradation, accumulation of damage, and its segregation (this study and refs. 10, 19, and 38). Note that in the case of modeling exponential growth of the cell we multiplied the extra term P_{int} by the growth rate of intact proteins:

$$\frac{dP_{\text{int}}}{dt} = \frac{P_{\text{int}} k_1}{k_s + P_{\text{int}} + P_{\text{dam}}} - k_2 P_{\text{int}} - k_3 P_{\text{int}} \quad [2]$$

The following set of transition equations describes how the proteins are distributed between progenitor and progeny when the cells divide; i.e., when P_{div} is reached.

For progenitors:

$$\begin{aligned}P(g+1) &= P_{\text{int}}(g)\cdot s_{\text{mother}} + P_{\text{dam}}(g)\cdot s_{\text{mother}}\\ P_{\text{dam}}(g+1) &= P_{\text{dam}}(g)\cdot s_{\text{mother}}\\ P_{\text{int}}(g+1) &= P_{\text{int}}(g)\cdot s_{\text{mother}}\end{aligned} \quad [3]$$

For progeny:

$$\begin{aligned}P(g+1) &= P_{\text{int}}(g)\cdot s_{\text{daughter}} + P_{\text{dam}}(g)\cdot s_{\text{daughter}}\\ P_{\text{dam}}(g+1) &= P_{\text{dam}}(g)\cdot s_{\text{daughter}}\\ P_{\text{int}}(g+1) &= P_{\text{int}}(g)\cdot s_{\text{daughter}}\end{aligned} \quad [4]$$

The size of the progenitor, s_{mother}, denotes the percentage of protein from the previous generation that is kept in that cell, whereas the size of the progeny, $s_{daughter}$, expresses the percentage of protein assigned to the newborn cell. $P(g + 1)$ denotes the initial amount of total protein for the new generation ($g + 1$),

Downloaded at Palestinian Territory, occupied on December 31, 2021
www.manaraa.com

whereas $P(g)$ corresponds to the final protein amount before division of the previous generation g.

We next introduced a retention coefficient (re), describing the amount of P_{dam} being retained by the progenitor. In this case, segregation of P_{dam}, and consequently P_{int}, is affected by both size and retention, according to the following set of transition equations:

For progenitor:

$$\begin{aligned} P(g+1) &= P_{int}(g)\cdot s_{mother} + P_{dam}(g)\cdot s_{mother} \\ P_{dam}(g+1) &= P_{dam}(g)\cdot(s_{mother} + (1 - s_{mother})\cdot re) \\ P_{int}(g+1) &= P_{int}(g)\cdot s_{mother} - P_{dam}(g)\cdot re\cdot(1 - s_{mother}) \end{aligned} \quad [5]$$

For progeny:

$$\begin{aligned} P(g+1) &= P_{int}(g)\cdot s_{daughter} + P_{dam}(g)\cdot s_{daughter} \\ P_{dam}(g+1) &= P_{dam}(g)\cdot s_{daughter}\cdot(1 - re) \\ P_{int}(g+1) &= P_{int}(g)\cdot s_{daughter} + P_{dam}(g)\cdot s_{daughter}\cdot re \end{aligned} \quad [6]$$

The values for retention range from $re = 0$ when the distribution of P_{dam} depends only on the size of the cell (see Eqs. **2** and **3**) to $re = 1$, when all P_{dam} is retained by the mother. We used the widely accepted assumption that the cell volume is proportional to the total amount of protein (P in our model). The increase in P_{dam}/P_{int} is different in the 2 siblings in the asymmetric model because of their different initial conditions (same ratio P_{dam}/P_{int} but different amounts of P_{dam} and P_{int}). P_{div} is not differently affected because this quantity is set in the model, but the time to reach P_{div} and the value of P_{dam}/P_{int} at this point are affected.

When simulating the different scenarios (Fig. 1 and Fig. S2), we recorded the fate of the progenitor and the progeny separately over a number of generations. We could therefore draw a ''parental lineage'' and an ''offspring lineage'' allowing us to follow, respectively, the next generation of mothers only, or the next generation of daughters only. To estimate the fitness of the whole population, we calculated and combined the number of divisions per unit time derived from each lineage.

Verification of the robustness of the system shows that changing the degradation rates of intact (k_2) and damaged (k_4) proteins yields comparable results (simulation results are not shown). An increased rate of degradation of damaged proteins (k_4), such that $k_2 < k_4$, results in progeny that never undergo replicative senescence, whereas their progenitors can cope with higher damage rates (k_3). Conversely, an increased degradation rate of intact proteins ($k_2 > k_4$) negatively affects the fitness and their capability to sustain higher damage rates of progenitors and progeny alike. Both reach replicative and clonal senescence much earlier (at $k_3 = 0.7$).

All numerical simulations that follow individual time courses were carried out by using Mathematica 5.2, Wolfram Research (39). To calculate the population size we used a custom Perl-script (www.perl.org) and SBML-PET (40).

ACKNOWLEDGMENTS. We thank Per Sunnerhagen (CMB, Gothenburg University, Sweden) for advice and providing the *S. pombe* strains used in this work and Axel Kowald (Ruhr-University, Bochum, Germany) for initial discussion. This work was supported by grants from the Swedish Natural Research Council, the Göran Gustafsson Foundation, and the European Commission (Contract 518230, Acronym: Proteomage). Part of the work of E.K. was supported by the European Commission (Contract MEST-CT2004–514169, Marie Curie Early Stage Training in Systems Biology; Contract 018942, Yeast Systems Biology Network).

1. Kirkwood TBL (1977) Evolution of ageing. *Nature* 270:301–304.
2. Medvedev ZA (1981) On the immortality of the germ cell line. *Int J Dev Biol* 42:1037–1042.
3. Kirkwood TB, Holliday R (1979) The evolution of ageing and longevity. *Proc R Soc Lond Ser B* 205:531–546.
4. Sheldrake AR (1974) The ageing, growth and death of cells. *Nature* 250:381.
5. Holliday R (1975) Growth and death of diploid and transformed human fibroblasts. *Fed Proc* 34:51–55.
6. Hernebring M, Brolen G, Aguilaniu H, Semb H, Nyström T (2006) Elimination of damaged proteins during differentiation of embryonic stem cells. *Proc Natl Acad Sci USA* 103:7700–7705.
7. Woldringh CL, Fluiter K, Huls PG (1995) Production of senescent cells of *Saccharomyces cerevisiae* by centrifugal elutriation. *Yeast* 11:361–369.
8. Sinclair DA, Guarente L (1997) Extrachromosomal rDNA circles—a cause of aging in yeast. *Cell* 91:1033–1042.
9. McMurray MA, Gottschling DE (2003) An age-induced switch to a hyper-recombinatorial state. *Science* 301:1908–1911.
10. Aguilaniu H, Gustafsson L, Rigoulet M, Nyström T (2003) Asymmetric inheritance of oxidatively damaged proteins during cytokinesis. *Science* 299:1751–1753.
11. Kennedy BK, Austriaco NR, Jr, Guarente L (1994) Daughter cells of *Saccharomyces cerevisiae* from old mothers display a reduced life span. *J Cell Biol* 127:1985–1993.
12. Erjavec N, Larsson L, Grantham J, Nyström T (2007) Accelerated aging and failure to segregate damaged proteins in Sir2 mutants can be suppressed by overproducing the protein aggregation-remodeling factor Hsp104p. *Genes Dev* 21:2410–2421.
13. Erjavec N, Nyström T (2007) Sir2p-dependent protein segregation gives rise to a superior reactive oxygen species management in the progeny of *Saccharomyces cerevisiae*. *Proc Natl Acad Sci USA* 104:10877–10881.
14. Ackermann M, Stearns SC, Jenal U (2003) Senescence in a bacterium with asymmetric division. *Science* 300:1920.
15. Stewart EJ, Madden R, Paul G, Taddei F (2005) Aging and death in an organism that reproduces by morphologically symmetric division. *PLoS Biol* 3:e45.
16. Nyström T (2007) A Bacterial Kind of Aging. *PLoS Genet* 3(12):e224.
17. Stadtman ER (1992) Protein oxidation and aging. *Science* 257:1220–1224.
18. Miller CG (1987) Protein degradation and proteolytic modification. *Escherichia coli and Salmonella typhimurium*: *Cellular and Molecular Biology*, ed Neidhardt FC (Am Soc for Microbiol, Washington, DC), pp 680–691.
19. Elliott SG, McLaughlin CS (1978) Rate of macromolecular synthesis through the cell cycle of the yeast *Saccharomyces cerevisiae*. *Proc Natl Acad Sci USA* 75:4384–4388.
20. Mitchison JM, Nurse P (1985) Growth in cell length in the fission yeast *Schizosaccharomyces pombe*. *J Cell Sci* 75:357–376.
21. Hayflick L, Moorhead P (1961) The serial cultivation of human diploid cell strains. *Exp Cell Res* 25:585–621.
22. Ackerman M, Chao L, Bergstrom CT, Doebeli M (2007) On the evolutionary origin of aging. *Aging Cell* 6:235–244.
23. Watve M, Parab S, Jogdand P, Keni S (2006) Aging may be a conditional strategic choice and not an inevitable outcome for bacteria. *Proc Natl Acad Sci USA* 103:14831–14835.
24. Martin SG, Chang F (2005) New end take off, regulating cell polarity during the fission yeast cell cycle. *Cell Cycle* 4:1046–1049.
25. Mata J, Nurse P (1997) Tea1 and the microtubular cytoskeleton are important for generating global special order within the fission yeast cell. *Cell* 89:939–949.
26. Glynn JM, Lustig RJ, Berlin A, Chang F (2001) Role of bud6p and tea1p in the interaction between actin and microtubules for the establishment of cell polarity in fission yeast. *Curr Biol* 11(11):836–845.
27. Parrinello S, *et al*. (2003) Oxygen sensitivity severely limits the replicative lifespan of murine fibroblasts. *Nat Cell Biol* 5:741–747.
28. Possos JF, *et al*. (2007) Mitochondrial dysfunction accounts for the stochastic heterogeneity in telomere-dependent senescence. *PLoS Biol* 5:e110.
29. Partridge L, Barton NH (1993) Optimality, mutation and the evolution of ageing. *Nature* 362:305–311.
30. Kirkwood T (1981) Repair and its Evolution: Survival versus Reproduction. *Physiological Ecology*: *An Evolutionary Approach to Resource Use* (Blackwell, Oxford), Chapter 7.
31. Lindner AB, Madden R, Demarez A, Stewart EJ, Taddei F (2008) Asymmetric segregation of protein aggregates is associated with cellular aging and rejuvenation. *Proc Natl Acad Sci USA* 105:3076–3081.
32. Nasim A, Young P, Johnson BF (1989) *Molecular biology of the fission yeast*. (Academic, New York)
33. Leupold U (1970) Genetical methods for *Schizosaccharomyces pombe*. *Methods Cell Physiol* 4:169–177.
34. Alfa C, *et al*. (1993) Experiments with Fission Yeast: A Laboratory Course Manual. (Cold Spring Harbor Lab Press, Cold Spring Harbor, NY) ISBN 0-87969-424-6.
35. Rupes I, Jia Z, Young PG (1999) SspI promotes actin depolymerization and is involved in stress response and new end take-off control in fission yeast. *Mol Biol Cell* 10:1495–1510.
36. Fantes PA (1982) Dependency relations between events in mitosis in *Schizosaccharomyces pombe*. *J Cell Sci* 55:383–402.
37. Barker MG, Walmsley RM (1999) Replicative ageing in the fission yeast *Schizosaccharomyces pombe*. *Yeast* 15:1511–1518.
38. Pratt JM, *et al*. (2002) Dynamics of protein turnover, a missing dimension in proteomics. *Mol Cell Proteomics* 1:579–591.
39. Wolfram Research (2005) Mathematica (Wolfram, Champaign, IL), Version 5.2.
40. Zi Z, Klipp E (2006) SBML-PET: A systems biology markup language-based parameter estimation tool. *Bioinformatics* 22:2704–2705.

Downloaded at Palestinian Territory, occupied on December 31, 2021

www.manaraa.com